

1      **Spreadsheet Data Extractor (SDE): A Performance-Optimized, User-Centric Tool**  
2      **for Transforming Semi-Structured Excel Spreadsheets into Relational Data**  
3

4      ANONYMOUS AUTHOR(S)  
5  
6      SUBMISSION ID:  
7

8      Spreadsheets are widely used across domains, yet their human-oriented layouts (merged cells, hierarchical headers, multiple tables)  
9      hinder automated extraction. We present the Spreadsheet Data Extractor (SDE), a user-in-the-loop system that converts semi-structured  
10     sheets into structured outputs without programming. Users declare the structure they perceive; the engine broadcasts selections  
11     deterministically and renders results immediately. Under the hood, SDE employs incremental loading, byte-level XML streaming  
12     (avoiding DOM materialisation), and viewport-bounded rendering.  
13

14     Optimised for time-to-first-visual, SDE delivers about **70 $\times$**  speedup over Microsoft Excel when opening a selected sheet in a large  
15     real-world workbook; under workload-equivalent conditions (single worksheet, full parse) it remains about **10 $\times$**  faster, while preserving  
16     layout fidelity. These results indicate SDE's potential for reliable, scalable extraction across diverse spreadsheet formats.  
17

18     CCS Concepts: • **Applied computing** → Spreadsheets; • **Information systems** → Data cleaning; • **Software and its engineering**  
19     → Extensible Markup Language (XML); • **Human-centered computing** → Graphical user interfaces; • **Theory of computation**  
20     → Data compression.  
21

22     Additional Key Words and Phrases: Spreadsheets, Data cleaning, Relational Data, Excel, XML, Graphical user interfaces  
23

24     **ACM Reference Format:**  
25

26     Anonymous Author(s). 2026. Spreadsheet Data Extractor (SDE): A Performance-Optimized, User-Centric Tool for Transforming  
27     Semi-Structured Excel Spreadsheets into Relational Data. In *Proceedings of Conference on Human Factors in Computing Systems (ACM*  
28     *CHI '26)*. ACM, New York, NY, USA, 25 pages. <https://doi.org/10.1145/XXXXXX.XXXXXXX>

29     **1 Introduction**  
30

31     Spreadsheets underpin workflows across healthcare [6], nonprofit organizations [17, 22], finance, commerce, academia,  
32     and government [11]. Despite their ubiquity, reliably analyzing and reusing the data they contain remains difficult  
33     for automated systems. In practice, many real-world spreadsheets are organized for human consumption [21] and  
34     therefore exhibit layouts with empty cells, merged regions, hierarchical headers, and multiple stacked tables. While  
35     such conventions aid human reading [16], they hinder machine readability and complicate extraction, integration, and  
36     downstream analytics.  
37

38     The reliance on spreadsheets as ad-hoc solutions poses several limitations:  
39

- 40     • **Data Integrity and Consistency:** Spreadsheets are prone to errors, such as duplicate entries, inconsistent  
41     data formats, and inadvertent modifications, which can compromise data integrity. [1, 8]  
42     • **Scalability Issues:** As datasets grow in size and complexity, spreadsheets become less efficient for data storage  
43     and retrieval, leading to performance bottlenecks. [15, 20]

---

45     Permission to make digital or hard copies of all or part of this work for personal or classroom use is granted without fee provided that copies are not  
46     made or distributed for profit or commercial advantage and that copies bear this notice and the full citation on the first page. Copyrights for components  
47     of this work owned by others than the author(s) must be honored. Abstracting with credit is permitted. To copy otherwise, or republish, to post on  
48     servers or to redistribute to lists, requires prior specific permission and/or a fee. Request permissions from [permissions@acm.org](mailto:permissions@acm.org).  
49

50     © 2025 Copyright held by the owner/author(s). Publication rights licensed to ACM.  
51

52     Manuscript submitted to ACM  
53

54     Manuscript submitted to ACM

- **Limited Query Capabilities:** Unlike databases, spreadsheets lack advanced querying and indexing features, restricting users from performing complex data analyses.

Transitioning from these ad-hoc spreadsheet solutions to standardized database systems offers numerous benefits:

- **Enhanced Data Integrity:** Databases enforce data validation rules and constraints, ensuring higher data quality and consistency.
- **Improved Scalability:** Databases are designed to handle large volumes of data efficiently, supporting complex queries and transactions without significant performance degradation.
- **Advanced Querying and Reporting:** Databases provide powerful querying languages like SQL, enabling sophisticated data analysis and reporting capabilities.
- **Seamless Integration:** Databases facilitate easier integration with various applications and services, promoting interoperability and data sharing across platforms.

Given the abundance of spreadsheet data and the clear advantages of database systems, there is a pressing need for tools that bridge these formats. Automated, accurate extraction from spreadsheets into relational representations is essential.

Prior work introduced a tool for extracting data from Excel files [4]. While effective, that system exhibited performance issues on large workbooks and imprecise rendering of cell geometry, which limited usability for complex, real-world files. The user interface was also fragmented, requiring context switches between hierarchy definition and output preview.

This paper presents the *Spreadsheet Data Extractor (SDE)* [3], which transforms data from semi-structured spreadsheets into machine-readable form. Users declare structure directly via cell selections—no programming is required. The design addresses the above limitations and supports large, irregular spreadsheets with predictable, interactive performance.

## 1.1 Contributions

- (1) **Unified interaction.** SDE integrates the selection hierarchy, worksheet view, and output preview into a single interface, reducing context switching and interaction count.
- (2) **DOM-free, byte-level worksheet parsing.** SDE implements a custom parser that operates directly on XLSX worksheet bytes, avoiding DOM construction and regular-expression passes over decoded strings; this substantially reduces memory footprint, parsing time, and improves robustness on large (“bloated”) sheets.
- (3) **Incremental loading.** Worksheets are loaded and parsed on demand from the XLSX archive, enabling near-instant open times and interactive latency on large files (quantified in 7. Evaluation).
- (4) **Excel-faithful rendering.** Row heights, column widths, and merged regions are recovered from the XML to render worksheets faithfully to Excel, improving user orientation.
- (5) **Viewport-bounded rendering.** The renderer draws only cells intersecting the viewport; selection queries are pruned with cached axis-aligned bounding boxes. Together these keep per-frame work proportional to what is visible rather than to sheet size.

## 2 Related Work

The extraction of relational data from semi-structured documents, particularly spreadsheets, has garnered significant attention due to their ubiquitous use across domains such as business, government, and scientific research. Several

Name	Technologies	Output	Accessibility	Frequency
DeExcelerator	heuristics	relational data	partially open source no access to GUI code	last publication 2015
FlashRelate	AI programming-by-example	relational data	proprietary, no access	last publication 2015
Senbazuru	AI	relational data	partially open source no access to GUI code	last commit 2015
XLIndy	AI	relational data	no access	discontinued
TableSense	AI	diagrams	proprietary, no access	last commit 2021
Aue et al. (converter)	User-centric Selection-Workflow	relational data	no public repository	last publication 2024

Table 1: Spreadsheet Data Extractor counterparts

frameworks and tools have been developed to address the challenges of converting flexible spreadsheet formats into normalized relational forms suitable for data analysis and integration as summarized in Table 1.

## 2.1 Aue et al.'s Converter

Aue et al. [4] developed a tool to facilitate data extraction from Excel spreadsheets by leveraging the Dart *excel* package [9] to process .xlsx files. This tool allows users to define data hierarchies by selecting relevant cells containing data and metadata. However, the approach faced significant performance bottlenecks due to the *excel* package's requirement to load the entire .xlsx file into memory, resulting in slow response times, particularly for large files.

In addition to memory issues, the tool calculated row heights and column widths based solely on cell content, ignoring the dimensions specified in the original Excel file. This led to rendering discrepancies between the tool and the original spreadsheet. Furthermore, the tool rendered all cells, regardless of their visibility within the viewport, significantly degrading performance when handling worksheets with large numbers of cells.

## 2.2 DeExcelerator

Eberius et al. [12] introduced **DeExcelerator**, a framework that transforms partially structured spreadsheets into first normal form relational tables using heuristic-based extraction phases. It addresses challenges such as table detection, metadata extraction, and layout normalization. While effective in automating normalization, its reliance on predefined heuristics limits adaptability to heterogeneous or unconventional spreadsheet formats, highlighting the need for more flexible approaches.

## 2.3 XLIndy

Koci et al. [13] developed **XLIndy**, an interactive Excel add-in with a Python-based machine learning backend. Unlike DeExcelerator's fully automated heuristic approach, XLIndy integrates machine learning techniques for layout inference and table recognition, enabling a more adaptable and accurate extraction process. XLIndy's interactive interface allows users to visually inspect extraction results, adjust configurations, and compare different extraction runs, facilitating iterative fine-tuning. Additionally, users can manually revise predicted layouts and tables, saving these revisions as annotations to improve classifier performance through (re-)training. This user-centric approach enhances the tool's

157 flexibility, allowing it to accommodate diverse spreadsheet formats and user-specific requirements more effectively  
158 than purely heuristic-based systems.  
159

## 160 2.4 FLASHRELATE

162 Barowy et al. [5] presented **FLASHRELATE**, an approach that empowers users to extract structured relational data from  
163 semi-structured spreadsheets without requiring programming expertise. FLASHRELATE introduces a domain-specific  
164 language, **FLARE**, which extends traditional regular expressions with spatial constraints to capture the geometric  
165 relationships inherent in spreadsheet layouts. Additionally, FLASHRELATE employs an algorithm that synthesizes  
166 FLARE programs from a small number of user-provided positive and negative examples, significantly simplifying the  
167 automated data extraction process.  
168

170 FLASHRELATE distinguishes itself from both DeExcelerator and XLIIndy by leveraging programming-by-example  
171 (PBE) techniques. While DeExcelerator relies on predefined heuristic rules and XLIIndy incorporates machine learning  
172 models requiring user interaction for fine-tuning, FLASHRELATE allows non-expert users to define extraction patterns  
173 through intuitive examples. This approach lowers the barrier to entry for extracting relational data from complex  
174 spreadsheet encodings, making the tool accessible to a broader range of users.  
175

## 177 2.5 Senbazuru

179 Chen et al. [7] introduced **Senbazuru**, a prototype Spreadsheet Database Management System (SSDBMS) designed to  
180 extract relational information from a large corpus of spreadsheets. Senbazuru addresses the critical issue of integrating  
181 data across multiple spreadsheets, which often lack explicit relational metadata, thereby hindering the use of traditional  
182 relational tools for data integration and analysis.  
183

184 Senbazuru comprises three primary functional components:  
185

186 (1) **Search**: Utilizing a textual search-and-rank interface, Senbazuru enables users to quickly locate relevant  
187 spreadsheets within a vast corpus. The search component indexes spreadsheets using Apache Lucene, allowing  
188 for efficient retrieval based on relevance to user queries.  
189

190 (2) **Extract**: The extraction pipeline in Senbazuru consists of several stages:

- 191 • **Frame Finder**: Identifies data frame structures within spreadsheets using Conditional Random Fields  
192 (CRFs) to assign semantic labels to non-empty rows, effectively detecting rectangular value regions and  
193 associated attribute regions.
- 195 • **Hierarchy Extractor**: Recovers attribute hierarchies for both left and top attribute regions. This stage  
196 also incorporates a user-interactive repair interface, allowing users to manually correct extraction errors,  
197 which the system then generalizes to similar instances using probabilistic methods.
- 199 • **Tuple Builder and Relation Constructor**: Generates relational tuples from the extracted data frames  
200 and assembles these tuples into coherent relational tables by clustering attributes and recovering column  
201 labels using external schema repositories like Freebase and YAGO.

202 (3) **Query**: Supports basic relational operations such as selection and join on the extracted relational tables, enabling  
203 users to perform complex data analysis tasks without needing to write SQL queries.  
204

205 Senbazuru's ability to handle hierarchical spreadsheets, where attributes may span multiple rows or columns without  
206 explicit labeling, sets it apart from earlier systems like DeExcelerator and XLIIndy. By combining learning methods  
207

209 with an interactive repair workflow, Senbazuru improves extraction accuracy and consistency and produces relations  
210 suitable for integration into databases.  
211

## 212 2.6 TableSense

213 Dong et al. [10] developed **TableSense**, an end-to-end framework for spreadsheet table detection using Convolutional  
214 Neural Networks (CNNs). TableSense addresses the diversity of table structures and layouts by introducing a compre-  
215 hensive cell featurization scheme, a Precise Bounding Box Regression (PBR) module for accurate boundary detection,  
216 and an active learning framework to efficiently build a robust training dataset.  
217

218 While **DeExcelerator**, **XLIndy**, **FLASHRELATE**, and **Senbazuru** focus primarily on transforming spreadsheet  
219 data into relational forms through heuristic, machine learning, and programming-by-example approaches, **TableSense**  
220 specifically targets the accurate detection of table boundaries within spreadsheets using deep learning techniques.  
221 Unlike region-growth-based methods employed in commodity spreadsheet tools, which often fail on complex table  
222 layouts, TableSense achieves superior precision and recall by leveraging CNNs tailored for the unique characteristics of  
223 spreadsheet data. However, TableSense focuses on table detection and visualization, allowing users to generate diagrams  
224 from the detected tables but does not provide functionality for exporting the extracted data for further analysis.  
225

## 226 2.7 Comparison and Positioning

227 A direct head-to-head comparison was not possible due to the lack of artifacts, because for the UI-oriented systems  
228 **FLASHRELATE**, **Senbazuru**, **XLIndy**, and **DeExcelerator**, we contacted the authors mentioned in the publications  
229 to obtain research artifacts (source code, UI prototypes). As of the submission deadline, we had either not received any  
230 responses or that the project was discontinued; we could not find publicly accessible UI artifacts or runnable packages.  
231

232 Moreover, unlike the aforementioned tools that rely on heuristics, machine learning, or AI techniques—which  
233 can introduce errors requiring users to identify and correct—we adopt a user-centric approach that gives users full  
234 control over data selection and metadata hierarchy definition. While this requires more manual input, it eliminates the  
235 uncertainty and potential inaccuracies associated with automated methods. To streamline the process and enhance  
236 efficiency, our tool includes user-friendly features such as the ability to duplicate hierarchies of columns and tables, and  
237 to move them over similar structures for reuse, reducing the need for repetitive configurations.  
238

239 By combining the strengths of manual control with enhanced user interface features and performance optimizations,  
240 our tool offers a robust and accessible solution for extracting relational data from complex and visually intricate  
241 spreadsheets. These enhancements not only improve performance and accuracy but also elevate the overall user  
242 experience, making our tool a valuable asset for efficient and reliable data extraction from diverse spreadsheet formats.  
243

## 244 3 Design Philosophy

245 Spreadsheet tables are heterogeneous, noisy, and locally structured in ways that are hard to infer reliably with fully  
246 automatic extraction. Our goal is not to replace the analyst with an opaque model, but to *amplify* their judgment: the  
247 user points to the structure they already perceive (regions, labels, value columns), and the system guarantees a faithful,  
248 auditable transformation into a relational view. Instead of automatically extracting and then searching for mistakes, we  
249 invert the workflow: *select first, broadcast deterministically, render immediately*. This keeps discrepancies visible at the  
250 point of selection, where they can be corrected with minimal context switches.  
251

252 We enforce three invariants: (i) **Provenance**: every emitted tuple is traceable to a set of visible source cells via  
253 an explicit mapping; (ii) **Stability**: small edits to selections induce bounded, predictable changes in the output (no  
254

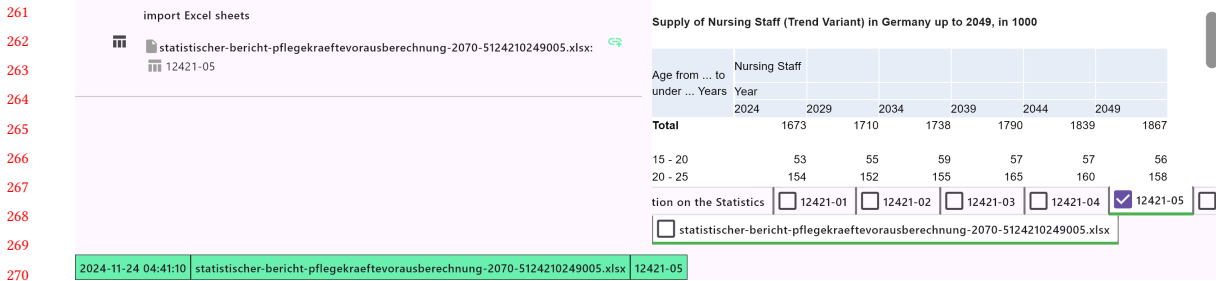


Fig. 1: The SDE Interface Overview.

global re-writes); (iii) **Viewport-bounded cost**: interactive operations run in time proportional to the number of cells intersecting the viewport, not the worksheet size. The parsing, indexing, and rendering subsystems are organized to uphold these invariants at scale.

*User-Centric Data Extraction.* The core interaction in the *SDE* lets users declare structure directly on the spreadsheet canvas and organize it into a hierarchy that drives a deterministic transformation into a relational view.

*Hierarchy Definition.* Users select individual cells or ranges (click, Shift-click for multi-selection). Each selection denotes either data (values) or metadata (labels/headers). Selections are arranged into a hierarchical tree: each node represents a data element; child nodes represent nested data or metadata. This hierarchy specifies how the *SDE* broadcasts selections into rows/columns in the output.

The interface supports flexible management: users drag-and-drop nodes to reparent or reorder the hierarchy when a different organization is more appropriate. Users can also introduce *custom nodes* with user-defined text to encode metadata that is implicit in the spreadsheet but absent from cell contents.

*Reusability and Efficiency.* To reduce repetitive work on sheets with repeated layouts, users can duplicate an existing selection hierarchy and apply it to similar regions. When moving a hierarchy, some cells may need to remain fixed (e.g., vertically stacked tables where only the topmost table repeats header rows). While in “move and duplicate” mode, the *SDE* provides a *lock* function: users freeze specific cells while relocating the rest of the hierarchy. Locks can be toggled via the lock icon at the top-left corner of a cell or next to the corresponding selection in the hierarchy panel; locked cells remain stationary while other selections shift accordingly (see Figure 4 in 4. Example Workflow). Already-locked selections are visually indicated and can be unlocked at any time.

#### 4 Example Workflow

Consider a spreadsheet containing statistical forecasts of future nursing staff availability in Germany [18]. Figure 1 shows the *SDE* interface, which consists of three main components:

**Hierarchy Panel (Top Left):** Displays the hierarchy of cell selections, initially empty.

**Spreadsheet View (Top Right):** Shows the currently opened Excel file and worksheet for cell selection.

**Output Preview (Bottom):** Provides immediate feedback on the data extraction based on current selections.

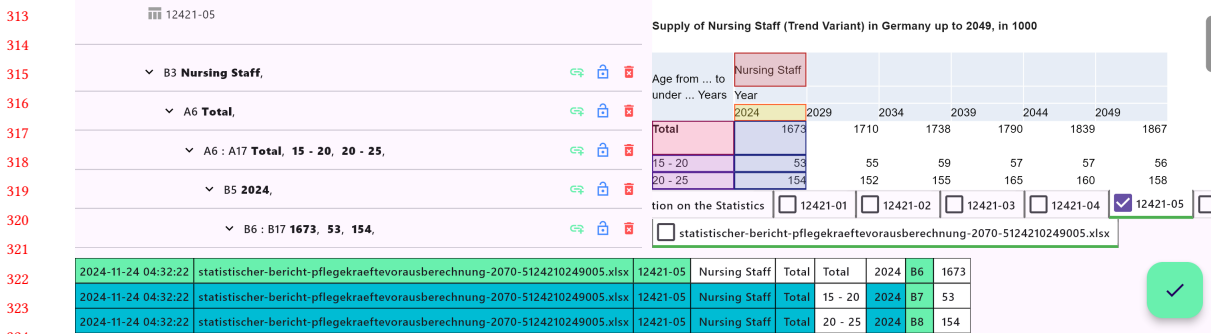


Fig. 2: Selection of the First Column Metadata

#### 4.1 Selection of the First Column

The user adds a node to the hierarchy and selects the cell containing the metadata "Nursing Staff" (Figure 2). This cell represents metadata that is common to all cells in this worksheet. Therefore, it should be selected first and should appear at the beginning of each row in the output CSV file.

Within this node, the user adds a child node and selects the cell "Total", which serves as both a table header and a row label. This selection represents the table header of the first subtable. The user adds another child node and selects the range of cells containing row labels (e.g., "Total", "15-20", "20-25" and so forth) by clicking the first cell and shift-clicking the last cell.

A further child node is then placed under the row labels node, and the user selects the year "2024". Subsequently, an additional child node is created beneath the year node, and the user selects the corresponding data cells (e.g., "1673", "53", "154", etc.).

At this point, the hierarchy consists of five nodes, each—except the last one—containing an embedded child node. In the upper-right portion of the interface, the chosen cells are displayed in distinct colors corresponding to each node. The lower area shows a preview of the extracted output. For each child node, an additional column is appended to the

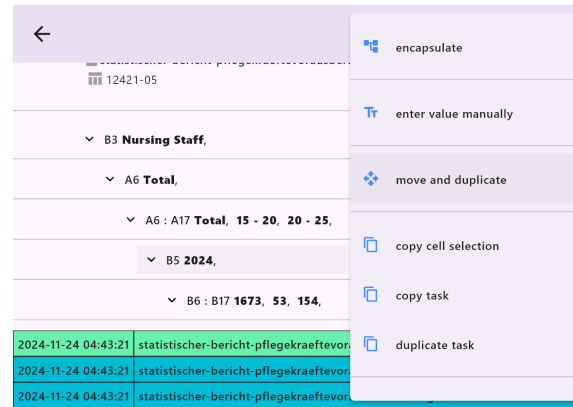


Fig. 3: Invoking the "move and duplicate" feature on the 2024 column node.

365  
366  
367  
368  
369 Supply of Nursing Staff (Trend Variant) in Germany up to 2049, in 1000  
370  
371 Age from ... to  
under ... Years Year  
372 2024 2029 2034 2039 2044 2049  
373 Total 1673 1710 1738 1790 1839 1867  
374 15 - 20 53 55 59 57 57 56  
20 - 25 154 152 155 165 160 158  
375

376 Fig. 4: Moving the hierarchy one cell to the right while adjusting the number of repetitions to duplicate the column  
377 selection.  
378

380 output. When multiple cells are selected for a given node, their values appear as entries in new rows of the output,  
381 reflecting the defined hierarchical structure.  
382

#### 383 4.2 Duplicating the Column Hierarchy

385 To avoid repetitive manual entry for additional years, the user duplicates the hierarchy for "2024" and adjusts the cell  
386 selections to include data for subsequent years (e.g., "2025," "2026") using the "Move and Duplicate" feature.  
387

388 To do this, the user selects the node of the first column "2024" and right-clicks on it. A popup opens in which the  
389 action "move and duplicate" appears, which should then be clicked, as shown in Figure 3.  
390

#### 391 4.3 Duplicating the Table Hierarchy

393 Subsequently, a series of buttons opens in the app bar at the top right, allowing the user to move the cell selections  
394 of the node as well as all child nodes, as seen in Figure 4. By pressing the button to move the selection by one unit  
395 to the right, the next column is selected. However, this would also deselect the first column since the selection was  
396 moved. To preserve the first column, the "move and duplicate" checkbox can be activated. This creates the shifted  
397 selection in addition to the original selection. The changes are only applied when the "accept" button is clicked. The next  
398 columns could also be selected in the same way. But this can be done faster, because instead of moving the selection and  
399 400

401  
402 12421-05  
403  
404 ✓ B3 Nursing Staff,     
405 ✓ A6 Total,     
406 ✓ A6 : A17 Total, 15 - 20, 20 - 25,     
407 ✓ B5 2024,     
408 ✓ B6 : B17 1673, 53, 154,     
409  
410  
411 2024-11-24 04:47:51 | statistischer-bericht-pflegekraeftevorausberechnung-2070-5124210249005.xlsx | 12421-05 | Nursing Staff | Total | Total | 2024 | B6 | 1673  
412 2024-11-24 04:47:51 | statistischer-bericht-pflegekraeftevorausberechnung-2070-5124210249005.xlsx | 12421-05 | Nursing Staff | Total | 15 - 20 | 2024 | B7 | 53  
413 2024-11-24 04:47:51 | statistischer-bericht-pflegekraeftevorausberechnung-2070-5124210249005.xlsx | 12421-05 | Nursing Staff | Total | 20 - 25 | 2024 | B8 | 154  
414  
415  
416

Supply of Nursing Staff (Trend Variant) in Germany up to 2049, in 1000

Age from ... to  
under ... Years Year  
2024 2029 2034 2039 2044 2049  
Total 1673 1710 1738 1790 1839 1867  
15 - 20 53 55 59 57 57 56  
20 - 25 154 152 155 165 160 158

tion on the Statistics  12421-01  12421-02  12421-03  12421-04  12421-05   
 statistischer-bericht-pflegekraeftevorausberechnung-2070-5124210249005.xlsx

Fig. 5: Resulting Hierarchy using the "Move and Duplicate" Function to Replicate the Column Selection Across Years

417 duplicating it only once, the "repeat" input field can be filled with as many repetitions as there are columns. By entering  
 418 the number 5, the selection of the first column is shifted 5 times by one unit to the right and duplicated at each step.  
 419

420 The user reviews the selections in the spreadsheet view, where each selection is highlighted in a different color  
 421 corresponding to its node in the hierarchy. Only after the user has reviewed the shifted and duplicated selections in  
 422 the worksheet and clicked the "accept" button are the nodes in the hierarchy created as desired. Figure 5 shows the  
 423 resulting selection after the user approved the proposed changes.  
 424

425 The same method that worked effectively for duplicating the columns can now be applied to the subtables, as shown  
 426 in Figure 6.

427 By selecting the node with the value "Total" and clicking the "Move and Duplicate" button, we can apply the selection  
 428 of the "Total" subtable to the other subtables. This involves shifting the table downward by as many rows as necessary  
 429 to overlap with the subtable below.  
 430

431 However, there is a minor issue: the child nodes of the "Total" node also include the column headers. If these column  
 432 headers were repeated in the subtables below, shifting the selections downward would work without modification.  
 433 Since these cells are not repeated in the subtables, we need to prevent the column headers cells from moving during the  
 434 duplication process.  
 435

Supply of Nursing Staff (Trend Variant) in Germany up to 2049, in 1000													
Age from ... to under ... Years		Year											
Age from ... to under ... Years		15	20	25	30	35	40	45	50	55	60	65	70
<b>Total</b>		1673	1710	1738	1790	1839	1867						
15 - 20		53	55	59	57	57	57	56					
20 - 25		154	152	155	165	160	160	158					
25 - 30		173	174	168	170	181	181	175					
30 - 35		178	186	184	178	180	180	191					
35 - 40		187	192	193	196	190	190	192					
40 - 45		175	201	204	209	207	207	201					
45 - 50		176	190	218	220	226	226	222					
50 - 55		177	177	193	225	228	228	233					
55 - 60		215	177	177	197	225	225	227					
60 - 65		166	170	139	140	156	156	178					
65 - 70		26	36	37	31	31	31	34					
<b>Male</b>		284	304	321	339	356	356	368					
15 - 20		12	13	14	13	13	13	13					
20 - 25		32	32	32	34	33	33	33					
25 - 30		39	40	39	39	39	41	40					
30 - 35		39	43	43	42	42	42	45					
35 - 40		38	42	46	46	44	44	45					
40 - 45		27	35	38	42	42	42	41					
45 - 50		24	26	35	38	41	41	41					
50 - 55		26	25	27	36	39	39	42					
55 - 60		25	25	25	27	35	35	39					
60 - 65		18	18	18	18	19	19	25					
65 - 70													
<b>Female</b>		1390	1406	1416	1451	1484	1484	1499					

466 Fig. 6: Selection of All Cells in the Subtables by Duplicating the Hierarchy of the First Table  
 467

To achieve this, we can exclude individual nodes from being moved by locking their selection. This is done by clicking the padlock icon on the corresponding nodes, which freezes their cell selection and keeps them fixed at their original position, regardless of other cells being moved.

Therefore, we identify and select the nodes containing the column headers—specifically, the years 2024 to 2049—and lock their selection using the padlock button. By shifting the selection downward and duplicating it, we can easily move and duplicate the cell selections for the subtables below. By setting the number of repetitions to 2, all subtables are completely selected.

#### 4.4 Path-wise Broadcasting

Figure 7 shows the selection hierarchy that users create on the spreadsheet. For readability, the example restricts itself to the first three columns and rows of the leftmost sub-table.

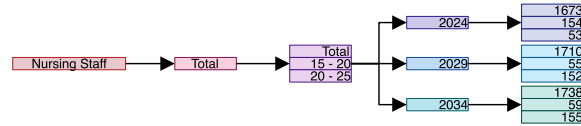


Fig. 7: Selection hierarchy before path-wise broadcasting.

To produce a flat, relational table, the SDE performs *path-wise broadcasting*: for each root-to-leaf path  $P = (v_0, \dots, v_k)$  that ends in a list of  $N$  value cells  $(x_1, \dots, x_N)$ , the SDE materializes  $N$  output rows by repeating or aligning the labels found along the path.

Concretely:

- (1) **Broadcast singletons.** If a path node carries a single label (e.g., *Nursing Staff*, *Total*, or a single year), that label is replicated  $N$  times so each value cell inherits it.
- (2) **Align equal-length lists.** If a path node provides a list of  $N$  labels, those labels are paired index-wise with the  $N$  value cells.
- (3) **Emit one tuple per value cell.** For each  $j \in \{1, \dots, N\}$ , emit a row that contains the labels gathered from the path at position  $j$  (broadcast or aligned) together with the value  $x_j$ .

The resulting hierarchy after broadcasting is illustrated in Figure 8: upstream labels are repeated or aligned so that each numeric cell is paired with its full context, yielding one relational row per cell.

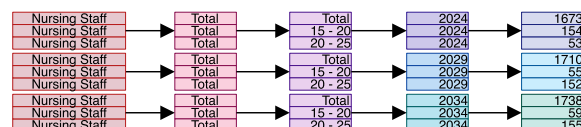


Fig. 8: Selection hierarchy after path-wise broadcasting. Each value cell is paired with its repeated/aligned upstream context, producing one row per cell.

## 5 Interface Fidelity for Navigation

To ensure that users can navigate worksheets without difficulty, we prioritize displaying the worksheets in a manner that closely resembles their appearance in Excel. This involves accurately rendering cell dimensions, formatting, and text behaviors.

**5.0.1 Displaying Row Heights and Column Widths.** Our solution extracts information about column widths and row heights directly from the Excel file's XML structure. Specifically, we retrieve the column widths from the *width* attribute of the *<col>* elements and the row heights from the *ht* attribute of the *<row>* elements in the *sheetX.xml* files.

In Excel, column widths and row heights are defined in units that do not directly correspond to pixels, requiring conversion for precise on-screen rendering. Moreover, different scaling factors are applied for columns and rows. Despite extensive research, we were unable to find official documentation that explains the rationale behind these specific scaling factors. Based on empirical testing, we derived the following scaling factors:

- **Column Widths:** Multiply the *width* attribute by 7.
- **Row Heights:** Multiply the *ht* attribute by  $\frac{4}{3}$ .

**5.0.2 Cell Formatting.** Cell formatting plays a crucial role in accurately representing the appearance of worksheets. Formatting information is stored in the *styles.xml* file, where styles are defined and later referenced in the *sheetX.xml* files as shown in Figure 9.

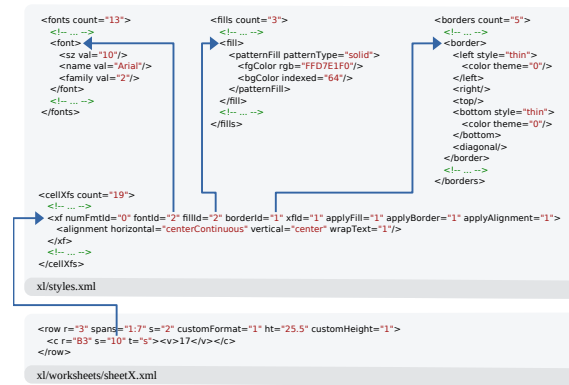


Fig. 9: Illustration of the relationship between style definitions in *xl/styles.xml* (fonts, fills, borders, and *cellXfs*) and their application in a worksheet file (*xl/worksheets/sheetX.xml*).

Each cell in the worksheet references a style index through the *s* attribute, which points to the corresponding *<xf>* element within the *cellXfs* collection. These *<xf>* elements contain attributes such as *fontId*, *fillId*, and *borderId*, which reference specific font, fill (background), and border definitions located in the *fonts*, *fills*, and *borders* collections, respectively. By parsing these references, we can accurately apply the appropriate fonts, background colors, and border styles to each cell.

Through meticulous parsing and application of these formatting details, we ensure that the rendered worksheet closely mirrors the original Excel file, preserving the visual cues and aesthetics that users expect.

**573** *5.0.3 Handling Text Overflow.* In Excel, when the content of a cell exceeds its width, the text may overflow into adjacent  
**574** empty cells, provided those cells do not contain any data. If adjacent cells are occupied, Excel truncates the overflowing  
**575** text at the cell boundary. Replicating this behavior is essential for accurate rendering and user familiarity.  
**576**

**577** We implemented text overflow handling by checking if the adjacent cell to the right is empty before allowing text to  
**578** overflow. If the adjacent cell is empty, we extend the text rendering. If the adjacent cell contains data, we truncate the  
**579** text at the boundary of the original cell.  
**580**

**581** Figure 1 illustrates this behavior. The text "Supply of Nursing Staff ..." extends into the neighboring cell because it is  
**582** empty. If not for this handling, the text would be truncated at the cell boundary, leading to incomplete data display as  
**583** shown in Figure 10.  
**584**

**585**

**586** [To the table of c](#)

**587**

**588** Supply of Nurs

**589**

Age from ... to under ... Years	Nursing Staff	Year	2024	2029	2034	2039	2044	2049	2049
Total			1673	1710	1738	1790	1839	1867	

**590**

**591**

**592**

**593**

**594** Fig. 10: Incorrect rendering without overflow for cells adjacent to empty cells.  
**595**

**596** By accurately handling text overflow, we improve readability and maintain consistency with Excel's user interface,  
**597** which is crucial for users transitioning between Excel and our tool.  
**598**

## **600** 6 Scalable Parsing, Indexing, and Rendering

**601** This section describes how the SDE achieves interactive performance on large or bloated worksheets: (i) *incremental*  
**602** loading of XLSX assets, (ii) a *byte-level worksheet parser* that avoids DOMs and regex, (iii) compact *indexes* for merged  
**603** regions and column geometry, (iv) *on-demand* streaming of rows and cells, and (v) *viewport-bounded* rendering.  
**604**

### **606** 6.1 Incremental Loading of Worksheets

**608** Opening large Excel files traditionally involves loading the entire file and all its worksheets into memory before  
**609** displaying any content. In files containing very large worksheets, this process can take several seconds to minutes,  
**610** causing significant delays for users who need to access data quickly.  
**611**

**612** To facilitate efficient data extraction from multiple Excel files, we implemented a mechanism for incremental loading  
**613** of worksheets within the SDE. Excel files (.xlsx format) are ZIP archives containing a collection of XML files that  
**614** describe the worksheets, styles, and shared strings. Key components include:  
**615**

- 616** • **x1/sharedStrings.xml**: Contains all the unique strings used across worksheets, reducing redundancy.
- 617** • **x1/styles.xml**: Defines the formatting styles for cells, including fonts, colors, and borders.
- 618** • **x1/worksheets/sheetX.xml**: Represents individual worksheets (sheet1.xml, sheet2.xml, etc.).  
**619**

**620** Our solution opens the Excel file as a ZIP archive and initially extracts only the essential metadata and shared  
**621** resources required for the application to function. This initial extraction includes:  
**622**

#### **623** (1) Metadata Extraction:

---

625 **Algorithm 1:** Backward search for </sheetData>

---

```

626 Input:  $b$ : bytes;  $[lo, hi]$ : search window
627 Output:  $sheetDataCloseByte$  or  $-1$ 
628 Function  $FindSheetDataEndBackward(b, lo, hi)$ :
629      $pat \leftarrow$  bytes of </sheetData>
630      $m \leftarrow |pat|$ 
631     for  $i \leftarrow hi - m$  downto  $lo$  do
632         if  $b[i] = pat[0]$  and  $b[i + m - 1] = pat[m - 1]$  and  $\text{EqualAt}(b, i, pat)$  then
633             return  $i$ 
634
635 return  $-1$ 

```

---

636 We read the archive’s directory to identify the contained files without decompressing them fully. This step is  
 637 quick, taking only a few milliseconds, and provides information about the available worksheets and shared  
 638 resources.  
 639

640 (2) **Selective Extraction:**

641 We immediately extract the `sharedStrings.xml` and the `styles.xml` files because these files are small and  
 642 contain information necessary for rendering cell content and styles across all worksheets. These files are parsed  
 643 and stored in memory for quick access during rendering.

644 (3) **Deferred Worksheet Loading:** The individual worksheet files (`sheetX.xml`) remain compressed and are  
 645 loaded into memory in their binary unextracted form. They are not decompressed or parsed at this stage.

646 (4) **On-Demand Parsing:**

647 When a user accesses a specific worksheet—either by selecting it in the interface or when a unit test requires  
 648 data from it—the corresponding `sheetX.xml` file is then decompressed and parsed. This parsing occurs in the  
 649 background and is triggered only by direct user action or programmatic access to the worksheet’s data.

650 (5) **Memory Release:**

651 After a worksheet has been decompressed and its XML parsed, we release the memory resources associated  
 652 with the parsed data. This approach prevents excessive memory usage and ensures that the application remains  
 653 responsive even when working with multiple large worksheets.

654 By adopting this incremental loading approach, users experience minimal wait times when opening an Excel file.  
 655 The initial loading is nearly instantaneous, allowing users to begin interacting with the application without delay. This  
 656 contrasts with traditional methods that require loading all worksheets upfront, leading to significant wait times for  
 657 large files.  
 658

## 6.2 Parsing Worksheet XML with Byte-Level Pattern Matching

659 DOM-based parsers and regex-on-strings do not scale for very large worksheets: they require full decoding to UTF-  
 660 16/UTF-8 and materialize enormous trees. In Dart, regular expressions cannot operate on byte arrays, so converting  
 661 a gigabyte-scale `Uint8List` to a string alone can cost seconds. The SDE therefore parses *directly on bytes*, matching  
 662 ASCII tag sentinels and reading attributes in place, decoding strings only on demand.

663 *Parsing roadmap.* Excel worksheets expose a stable top-level order: `<sheetFormatPr>`, `<cols>`, `<sheetData>`,  
 664 `<mergeCells>`. We first anchor the end of `<sheetData>` by a backward byte search; then we parse metadata around it:

- 665 • `<mergeCells>` (after `</sheetData>`),
- 666 • `<sheetFormatPr>` (before `<sheetData>`) and

- 677     • <cols> (before <sheetData>)

678 and enter *sheet-data mode* only when rows or cells are actually needed.

680     *Anchoring & metadata.* We find the closing </sheetData> sentinel by scanning backward and validating the 12-byte  
 681 pattern (Alg. 1). This yields byte indices that bound all subsequent searches and lets us enumerate <mergeCell ...  
 682 ref="A1:B3"> elements linearly, converting each A1 pair to  $(r, c)$  and inserting the span into a compact index with  
 683 binary-search probes and a prefix-maximum (used later by spanAt, Alg. 4).

686     *Defaults and column bands.* We record the default row height  $H_d$  (attribute defaultRowHeight) and the default  
 687 column width  $W_d$  (attribute defaultColWidth) in the <sheetFormatPr ...> node. From <cols> we parse each element  
 688 of the form <col min="i" max="j" width="w">, which defines a *column band*  $[i:j]$  with width  $w$ . Bands are stored  
 689 in ascending order of min; queries such as retrieving the width at column  $c$  or the column at a given horizontal offset  
 690 are answered via a linear or  $O(\log B)$  search over these bands.

693     *Streaming rows and accumulating offsets.* Entering sheet-data mode, we stream <row ...> tags without decoding  
 694 payloads. Within each opening tag we read  $r = \dots$  (row index) and  $ht = \dots$  (height) if present. For each discovered  
 695 row we cache its byte interval and compute its top offset incrementally using explicit heights or the default  $H_d$ :

$$697 \quad off_1 = (r_1 - 1) H_d, \quad off_i = off_{i-1} + (h_{i-1} \text{ or } H_d) + (r_i - r_{i-1} - 1) H_d.$$

699 See Alg. 2.

701     *Lazy cell parsing.* Given a row byte interval  $[s, e)$ , cells are parsed on demand. We scan for <c>, read attributes  
 702 ( $r = "A123"$ ,  $s = \dots$ ,  $t = \dots$ ), and bound the cell interval by the next <c> or the row end. Values are extracted *within*  
 703 this interval from <v>...</v> or (for inline strings) <is>...</is>. See Alg. 3. Because Excel enforces increasing row  
 704 indices, we can stop row streaming as soon as we pass the requested row.

707     *Merged regions.* Merged areas are rectangles  $[r_1, r_2] \times [c_1, c_2]$ . We normalize and sort spans by  $(r_1, c_1)$ , store parallel  
 708 arrays  $R_1, C_1, R_2, C_2$ , and build a prefix-maximum PM over  $R_2$ . A point query spanAt( $r, c$ ) uses (i) a binary search on  
 709  $R_1$  to cap candidates above  $r$ , (ii) a binary search over PM to drop candidates ending before  $r$ , (iii) a binary search on  $C_1$   
 710 to find those with  $c_1 \leq c$ , then a short local check; an origin map answers “is this cell the origin?” in  $O(1)$ . See Alg. 4.

712     *Scroll extents (without decoding payloads).* We obtain  $r_{\max}$  by scanning backward to the last <row ... r = "...>. A  
 713 single forward pass accumulates  $\sum_{r \in E} ht(r)$  and counts  $|E|$ ; all other rows use  $H_d$ . In device units,

$$715 \quad H_{\text{sheet}} = \sum_{r \in E} ht(r) + (r_{\max} - |E|) H_d.$$

718 Horizontally, letting  $c_{\max}$  be the largest covered column,

$$719 \quad W_{\text{sheet}} = \text{colOff}(c_{\max}) + w(c_{\max}).$$

721 These extents parameterize the viewport and drive scrollbar sizing in the UI.

723     *Complexity and memory.* All searches are bounded by structural sentinels (>, next <row>, next <c>, or </sheetData>).  
 724 Anchoring </sheetData> is  $O(N)$  with tiny constants; row streaming is  $O(R)$  with  $O(1)$  per-row offset updates; a  
 725 targeted cell within a row scans only that row’s interval; merge queries run in  $O(\log M + \alpha)$  with a short local scan  $\alpha$ .  
 726 The representation is compact (byte slices + small numeric state), and strings are decoded only when needed.

**Algorithm 2:** Stream rows & compute offsets

**Input:**  $b$ : bytes; window  $[o, c)$  with  $o = \text{index after } <\text{sheetData}>$ ,  $c = \text{index of } </\text{sheetData}>$ ; default height  $H_d$ ; pixel scale  $\rho$

**Output:** sequence of  $\langle r, [s, e), h, \text{off} \rangle$

**Function**  $\text{RowsWithOffsets}(b, [o, c), H_d, \rho)$ :

```

 $i \leftarrow o; \quad \text{prevR} \leftarrow \perp; \quad \text{prevH} \leftarrow \perp; \quad \text{prevOff} \leftarrow 0; \quad \text{prevS} \leftarrow \perp$ 
while  $i \leq c - 4$  do
    if  $b[i..i + 3] = <\text{row}>$  then
         $s \leftarrow i$ 
         $(r, h, j) \leftarrow \text{PARSEROWATTRS}(b, i, c)$  // advances to just after >
        if  $\text{prevR} = \perp$  then
             $\text{off} \leftarrow \rho \cdot (r - 1) H_d$ 
        else
             $g \leftarrow r - \text{prevR} - 1$ 
             $H_{\text{prev}} \leftarrow (\text{prevH or } H_d)$ 
             $\text{off} \leftarrow \text{prevOff} + \rho \cdot H_{\text{prev}} + \rho \cdot g H_d$ 
        if  $\text{prevR} \neq \perp$  then emit  $\langle \text{prevR}, [\text{prevS}, s), \text{prevH}, \text{prevOff} \rangle$ 
         $\text{prevR} \leftarrow r; \quad \text{prevH} \leftarrow h; \quad \text{prevOff} \leftarrow \text{off}; \quad \text{prevS} \leftarrow s$ 
         $i \leftarrow j$ 
    else
         $i \leftarrow i + 1$ 
if  $\text{prevR} \neq \perp$  then emit  $\langle \text{prevR}, [\text{prevS}, c), \text{prevH}, \text{prevOff} \rangle$ 

```

**Input:**  $b$ : bytes;  $i$ : index at  $<\text{row}$ ;  $c$ : close bound (sheet end)

**Output:**  $\langle r, h, j \rangle$ : row index  $r$  (or  $\perp$ ), optional height  $h$  (or  $\perp$ ), and  $j = \text{first byte after } >$

**Function**  $\text{ParseRowAttrs}(b, i, c)$ :

```

 $r \leftarrow \perp; \quad h \leftarrow \perp; \quad j \leftarrow i + 4$ 
while  $j < c$  do
    if  $b[j] = >$  then
         $j \leftarrow j + 1; \quad \text{return} (r, h, j)$ 
    if  $b[j] = r \text{ and } b[j - 1] \text{ is space}$  then
         $k \leftarrow j + 1$ 
         $(s, e) \leftarrow \text{GETINNERATTRINTERVAL}(k, c, b)$ 
        if  $(s, e) \neq \perp$  then  $r \leftarrow \text{PARSEINTASCII}(b, s, e)$ 
    if  $b[j..j + 1] = \text{ht} \text{ and } b[j - 1] \text{ is space}$  then
         $k \leftarrow j + 2$ 
         $(s, e) \leftarrow \text{GETINNERATTRINTERVAL}(k, c, b)$ 
        if  $(s, e) \neq \perp$  then  $h \leftarrow \text{PARSEDOUBLEASCII}(b, s, e)$ 
     $j \leftarrow j + 1$ 
return  $(r, h, j)$  // malformed tail safely falls through

```

**Input:**  $i$ : scan index after the attribute name;  $n$ : hard bound;  $b$ : bytes

**Output:**  $(s, e)$  inner half-open interval, or  $\perp$  if not well-formed

**Function**  $\text{GetInnerAttrInterval}(i, n, b)$ :

```

while  $i < n \text{ and } b[i] \text{ is space}$  do
     $i \leftarrow i + 1$ 
if  $i < n \text{ and } b[i] = =$  then
     $i \leftarrow i + 1$ 
    while  $i < n \text{ and } b[i] \text{ is space}$  do
         $i \leftarrow i + 1$ 
    if  $i < n \text{ and } (b[i] = " \text{ or } b[i] = ')$  then
         $q \leftarrow b[i]; i \leftarrow i + 1; s \leftarrow i$ 
        while  $i < n \text{ and } b[i] \neq q$  do
             $i \leftarrow i + 1$ 
        return  $(s, i)$ 
return  $\perp$ 

```

---

**Algorithm 3:** Resolve cell by streaming the row

---

```

781 Input:  $b$ : bytes; row interval  $[S, E)$ ; target column  $c$ 
782 Output: cell interval  $[s, e)$  or  $\perp$ 
783  $i \leftarrow S$ 
784 while  $i \leq E - 2$  do
785   if  $b[i..i + 1] = <c$  then
786      $s \leftarrow i$ 
787      $(c', j) \leftarrow \text{PARSECELLCOL}(b, i, E)$                                 // reads r="A123" and advances to just after >
788     // end of this cell = next <c or E
789      $k \leftarrow j$ 
790     while  $k \leq E - 2$  and  $b[k..k + 1] \neq <c$  do
791        $k \leftarrow k + 1$ 
792        $e \leftarrow (k \leq E - 2) ? k : E$ 
793       if  $c' = c$  then
794         return  $[s, e)$ 
795        $i \leftarrow e$ 
796     else
797        $i \leftarrow i + 1$ 
798
799 return  $\perp$ 
800

```

---

### 6.3 Two-Dimensional Grid Viewport Rendering

Given a (potentially very large) worksheet with variable row heights, banded column widths, and merged regions, we lay out only tiles intersecting the current viewport. The renderer works in device pixels but derives all positions from the byte-level parser. Our goal is *frame-local* work proportional to the number of *visible* rows/columns, independent of sheet size. Algorithm 4 summarizes the procedure. Throughout, index intervals are half-open  $[a, b)$ .

**Inputs.** Let  $x_0, y_0$  be the horizontal/vertical scroll offsets (device pixels) and  $W_{\text{vp}}, H_{\text{vp}}$  the viewport size. We use a small *cache extent*  $\Delta > 0$  to pre-build tiles that will imminently enter view, rendering over  $[x_0, x_0 + W_{\text{vp}} + \Delta] \times [y_0, y_0 + H_{\text{vp}} + \Delta]$ . Row geometry comes from the streaming parser: each row  $r$  has a top offset  $\text{off}(r)$  and a height  $h(r)$  (explicit *ht* if present, otherwise the default). Columns are given as ordered bands; for column  $c$  we can query its width  $w(c)$  and cumulative offset  $\text{colOff}(c)$ . Merged regions are indexed by a structure that decides, in logarithmic time, whether a coordinate  $(r, c)$  is covered and, if so, by which span.

**Visible set.** We invert the cumulative-height/width functions:

$$\begin{aligned} r_l &= \lfloor \text{rowIndexAt}(y_0) \rfloor, & r_u &= \lceil \text{rowIndexAt}(y_0 + H_{\text{vp}} + \Delta) \rceil, \\ c_l &= \lfloor \text{colIndexAt}(x_0) \rfloor, & c_u &= \lceil \text{colIndexAt}(x_0 + W_{\text{vp}} + \Delta) \rceil. \end{aligned}$$

Here  $\text{rowIndexAt}(y)$  and  $\text{colIndexAt}(x)$  are binary searches over cumulative extents built from parsed row heights and column bands, yielding  $O(\log R)$  and  $O(\log B)$  lookup time, respectively.

**Cell coordinates and merge spans.** A merged region is a closed rectangle  $[r_1, r_2] \times [c_1, c_2]$  with  $r_1 \leq r_2$  and  $c_1 \leq c_2$ . We sort spans by origin  $(r_1, c_1)$  and materialize parallel arrays  $R_1, C_1, R_2, C_2$  plus a prefix-maximum array  $\text{PM}[i] = \max_{0 \leq j \leq i} R_2[j]$ . An origin map supports  $O(1)$  checks that  $(r, c)$  is the top-left of a span. Membership “is  $(r, c)$  covered?” runs in three bounded steps:

- (1) **Row window (binary search).**  $hi = \text{ub}(R_1, r)$ ; candidates lie in  $[0, hi)$ . Then  $lo = \text{lb}(\text{PM}[0:hi], r)$  discards all indices with  $R_2 < r$ .
- (2) **Column narrowing (binary search).**  $k = \text{ub}(C_1[lo:hi], c) - 1$  is the last origin with  $c_1 \leq c$ .

**Algorithm 4:** Viewport layout with merge-aware origin-first placement

**Input:**  $x_0, y_0; W_{vp}, H_{vp}$ ; cache  $\Delta$ ; sheet accessors  $\text{rowIndexAt}, \text{colIndexAt}, \text{off}, \text{colOff}, h, w$ ; merge index  $\text{spanAt}, \text{isOrigin}$   
**Output:** positioned tiles for current frame

```

833 // Visible indices
834  $r_l \leftarrow [\text{rowIndexAt}(y_0)], r_u \leftarrow [\text{rowIndexAt}(y_0 + H_{vp} + \Delta)]$ 
835  $c_l \leftarrow [\text{colIndexAt}(x_0)], c_u \leftarrow [\text{colIndexAt}(x_0 + W_{vp} + \Delta)]$ 
836  $B \leftarrow \emptyset // burned merged spans$ 
837
838 // Pass 1: top border probes
839 for  $c \leftarrow c_l$  to  $c_u$  do
840    $S \leftarrow \text{spanAt}(r_l, c)$ 
841   if  $S \neq \perp$  and  $S \notin B$  and  $r_S < r_l$  then
842     place tile for  $S$  at  $(\text{colOff}(c_S) - x_0, \text{off}(r_S) - y_0)$ 
843      $B \leftarrow B \cup \{S\}$ 
844
845 // Pass 2: left border probes
846 for  $r \leftarrow r_l$  to  $r_u$  do
847    $S \leftarrow \text{spanAt}(r, c_l)$ 
848   if  $S \neq \perp$  and  $S \notin B$  and  $c_S < c_l$  then
849     place tile for  $S$  at  $(\text{colOff}(c_S) - x_0, \text{off}(r_S) - y_0)$ 
850      $B \leftarrow B \cup \{S\}$ 
851
852 // Pass 3: interior tiles
853 for  $c \leftarrow c_l$  to  $c_u$  do
854    $x \leftarrow \text{colOff}(c) - x_0$ 
855   for  $r \leftarrow r_l$  to  $r_u$  do
856      $y \leftarrow \text{off}(r) - y_0$ 
857      $S \leftarrow \text{spanAt}(r, c)$ 
858     if  $S = \perp$  or  $\text{isOrigin}(S, (r, c))$  then
859       place tile at  $(x, y)$ 
860
861 Function  $\text{spanAt}(r, c)$ :
862    $hi \leftarrow \text{ub}(R_1, r)$ 
863   if  $hi = 0$  then
864     return  $\perp$ 
865    $lo \leftarrow \text{lb}(PM[0:hi], r)$ 
866   if  $lo \geq hi$  then
867     return  $\perp$ 
868    $k \leftarrow \text{ub}(C_1[lo:hi], c) - 1$ 
869   if  $k < lo$  then
870     return  $\perp$ 
871   for  $i \leftarrow k$  downto  $lo$  do
872     if  $C_1[i] > c$  then
873       break
874     if  $r \leq R_2[i]$  and  $c \leq C_2[i]$  then
875       return  $\text{span } i$ 
876
877 return  $\perp$ 

```

(3) **Local check (constant expected).** Scan left from  $k$  while  $C_1[i] \leq c$ ; accept if  $r \leq R_2[i]$  and  $c \leq C_2[i]$ .

We use  $\text{ub}(A, x) = \min\{i \mid A[i] > x\}$  and  $\text{lb}(A, x) = \min\{i \mid A[i] \geq x\}$ . This yields  $O(\log M + \alpha)$  time, where  $\alpha$  is a short local scan in practice.

*Origin-first placement for merged regions.* A naïve scan of  $[r_l : r_u] \times [c_l : c_u]$  would instantiate merged tiles multiple times. Instead, we *pre-place* only spans whose origins lie outside the leading edges but whose rectangles intersect the viewport: probe the top border  $(r_l, c_l : c_u)$  and the left border  $(r_l : r_u, c_l)$ , query  $\text{spanAt}(r, c)$ , and place the tile once at its origin  $(r_S, c_S)$ . We maintain a burned set  $B$  to avoid duplicates in the interior.

---

**Algorithm 5:** AABB-indexed selection lookup over visible grids

---

```

885 Input: point  $(x, y)$ ; arrays  $L, R, T, B$ ; permutation  $\sigma$  sorting by  $T$ ; prefix max PM over  $B_{\sigma(\cdot)}$ ; original-order  $O$ ; accessor  $\text{findCell}_i(x, y)$ 
886 Output: either  $\langle i, \text{cell} \rangle$  or  $\perp$ 
887 // Binary-search helpers:  $\text{ub}(A, z) = \min\{i \mid A[i] > z\}$ ,  $\text{lb}(A, z) = \min\{i \mid A[i] \geq z\}$ .
888 // 1) Y-narrowing: window of candidates whose top  $\leq y$  and bottom  $\geq y$ 
889  $h \leftarrow \text{ub}(T_\sigma, y)$   $\perp$  // first index with  $T_{\sigma(h)} > y$ 
890 if  $h = 0$  then
891    $\perp$ 
892  $\ell \leftarrow \text{lb}(\text{PM}[0:h], y)$   $\perp$  // first prefix with bottom  $\geq y$ 
893 if  $\ell \geq h$  then
894    $\perp$ 
895 // 2) X-pruning: keep only boxes covering  $x$ 
896  $\mathcal{C} \leftarrow \emptyset$ 
897 for  $j \leftarrow \ell$  to  $h - 1$  do
898    $i \leftarrow \sigma(j)$ 
899   if  $L_i \leq x \leq R_i$  then
900      $\perp$  append  $i$  to  $\mathcal{C}$ 
901 if  $\mathcal{C} = \emptyset$  then
902    $\perp$ 
903 // 3) Stable tie-break and confirmation
904  $\mathcal{C} \leftarrow \text{sort } \mathcal{C} \text{ by increasing } O_i$   $\perp$  // preserve UI order/colors
905 foreach  $i \in \mathcal{C}$  do
906    $ans \leftarrow \text{findCell}_i(x, y)$ 
907   if  $ans \neq \perp$  then
908      $\perp$   $\langle i, ans \rangle$ 
909 return  $\perp$ 
910
911
912
913
914
915
916
917
918
919
920
921
922
923
924
925
926
927
928
929
930
931
932
933
934
935
936

```

---

909 *Interior tiling.* Traverse the visible grid and place a tile at  $(r, c)$  only if (i) no span covers it, or (ii)  $(r, c)$  is the origin of  
910 its span (checked in  $O(1)$ ). Device positions are  $x = \text{colOff}(c) - x_0$ ,  $y = \text{off}(r) - y_0$ .

912 *Scroll extents.* We size the vertical scroll domain from row attributes without decoding payloads. Anchored at  
913  $</\text{sheetData}>$ , we scan backward to the last  $<\text{row} \dots>$  to read  $r_{\max}$  from  $r=" \dots "$ . A single forward pass accumulates  
914 explicit heights  $\sum_{r \in E} \text{ht}(r)$  and counts them as  $|E|$ ; all other rows in  $1..r_{\max}$  use the default  $H_d$ . With device pixels,  
915

$$H_{\text{sheet}} = \sum_{r \in E} \text{ht}(r) + (r_{\max} - |E|) H_d.$$

916 Horizontally, with  $c_{\max}$  the highest covered column,

$$W_{\text{sheet}} = \text{colOff}(c_{\max}) + w(c_{\max}).$$

917 These extents parameterize the viewport and drive scrollbar sizing/positioning (*two\_dimensional\_scrollables* [14]).

918 *Correctness and complexity.* Edge probes ensure any merged region intersecting the viewport but originating above/left  
919 is instantiated *exactly once* at its origin. The interior pass either places unmerged cells or the unique origin cell of each  
920 merged region. Let  $R_{\text{vis}} = r_u - r_l + 1$  and  $C_{\text{vis}} = c_u - c_l + 1$ . Passes 1-2 cost  $O(R_{\text{vis}} + C_{\text{vis}})$ ; Pass 3 costs  $O(R_{\text{vis}} C_{\text{vis}})$  and  
921 does no work outside the visible rectangle. The burned set is updated at most once per span per frame.

#### 922 6.4 AABB-Indexed Selection Lookup

923 Each selection source (a task or composed group) maintains a lazily computed, cached *axis-aligned bounding box*  
924 (AABB) that is invalidated on updates and recomputed on demand (Algorithm 5). When many such selection sources  
925 (grids) intersect the viewport, a linear scan over their bounding boxes can dominate latency. We therefore maintain a  
926 Manuscript submitted to ACM

---

**Algorithm 6:** Lazy row locator: driver and lookup (part A)
 

---

```

937 Input: hierarchy files→tasks→sheets→cellTasks; caps  $B_{\max}, R_{\max}$ 
938 Output: on demand: for global row  $r$ , return (RowBlock, local) or  $\perp$ 
939 State: arrays  $blocks, starts$ ; queue  $Q$ ; indices  $fi, sti, si; curFile, curTask, curSheets; (activeWb, activeSheet)$ .
940 Function EnsureBuiltThroughRow( $r$ ):
941   while  $builtRows \leq r$  do
942      $rb \leftarrow \text{NextBlock}()$ 
943     if  $rb = \perp$  then
944        $\perp$  break
945     append  $rb$  to  $blocks$ ; append  $rb.startRow$  to  $starts$ ;
946     PruneHeadIfNeeded()
947 Function LocateRow( $r$ ):
948   EnsureBuiltThroughRow( $r$ )
949   if  $blocks = \emptyset$  then
950      $\perp$ 
951    $lo \leftarrow 0; hi \leftarrow |starts|$ 
952   while  $lo < hi$  do
953      $mid \leftarrow \lfloor (lo + hi)/2 \rfloor$ 
954     if  $starts[mid] \leq r$  then
955        $lo \leftarrow mid + 1$ 
956     else
957        $hi \leftarrow mid$ 
958      $idx \leftarrow lo - 1$ 
959     if  $idx < 0$  then
960        $\perp$ 
961      $b \leftarrow blocks[idx]; local \leftarrow r - b.startRow$ 
962     if  $0 \leq local < b.len$  then
963        $\perp$ 
964     else
965        $\perp$ 
966 
```

---

lightweight index over axis-aligned bounding boxes (AABBs) to answer point queries  $(x, y)$  in  $O(\log G + \alpha)$  time, where  $G$  is the number of visible grids and  $\alpha$  is the size of a narrow candidate window. their bounding boxes can dominate latency. We therefore maintain a lightweight index over axis-aligned bounding boxes (AABBs) to answer point queries  $(x, y)$  in  $O(\log G + \alpha)$  time, where  $G$  is the number of visible grids and  $\alpha$  is the size of a narrow candidate window.

Each grid  $i$  exposes a bounding rectangle  $[L_i, R_i] \times [T_i, B_i]$  in grid coordinates and a point predicate  $\text{findCell}_i(x, y)$  that returns the cell at  $(x, y)$  or  $\perp$ . We build parallel arrays  $L, R, T, B$  (left, right, top, bottom) and a stable original-order index  $O$  (used to break ties consistently with the UI). Let  $\sigma$  be the permutation that sorts grids by nondecreasing  $T$  (top edge). In that order we form a prefix-maximum array  $\text{PM}[j] = \max_{0 \leq i \leq j} B_{\sigma(i)}$ . For a query row  $y$ , the candidate window is the tightest interval  $[\ell, h]$  such that all boxes whose top  $\leq y$  and bottom  $\geq y$  lie in that interval; we obtain  $h = \text{ub}(T_\sigma, y)$  and  $\ell = \text{lb}(\text{PM}[0:h], y)$  by binary search (ub: strict upper bound; lb: lower bound). We then prune by the  $x$ -interval condition  $L \leq x \leq R$ . Among the surviving candidates we test  $\text{findCell}$  in increasing  $O$  (original) order and return the first hit; if none match, the answer is  $\perp$ .

The index builds in  $O(G \log G)$  time and consists of six integer arrays plus the permutation  $\pi$ . It is invalidated on any structural change to the set of grids (move, resize, insert/delete) and rebuilt lazily on the next query. For small  $G$  (e.g.,  $G \leq 32$ ) we fall back to a linear scan; the cutover can be tuned empirically.

**Streaming next block.** NEXTBLOCK (Alg. 7) emits the next contiguous block. If  $Q$  is empty we call FILLQUEUEIFEMPTY to advance to the next *source segment* (file, sheet task, sheet pair) with non-empty roots. Otherwise we pop a frame. If the popped task has no children, its sortedSelectedCells form a new RowBlock ( $\text{start} = \text{builtRows}$ , length =

989 number of selected cells) and we return it. If the task has children, we enqueue each child with the extended path. This  
 990 BFS over the selection tree yields a deterministic, top-down order that matches the user's mental model.  
 991

992

---

**Algorithm 7:** Row block generation (part B): NextBlock
 

---

```

994 Function NEXTBLOCK:
995   if  $\neg \text{FillQueueIsEmpty}()$  then
996      $\quad \text{return } \perp$ 
997   while true do
998     if  $Q = \emptyset$  then
999       if  $\neg \text{FillQueueIsEmpty}()$  then
1000          $\quad \text{return } \perp$ 
1001       continue
1002      $(t, path) \leftarrow \text{pop-front } Q$ 
1003     if  $t.\text{children} = \emptyset$  then
1004        $cells \leftarrow t.\text{sortedSelectedCells}$ 
1005       if  $|cells| = 0$  then
1006          $\quad \text{continue}$ 
1007        $start \leftarrow \text{builtRows}; len \leftarrow |cells|$ 
1008        $\text{return } \text{RowBlock}(activeWb, activeSheet, path, cells, start, len)$ 
1009
1010      $nextPath \leftarrow path \cup \{t\}$ 
1011     foreach  $u \in t.\text{children}$  do
1012       push-back  $(u, nextPath)$  into  $Q$ 
  
```

---

1009

1010

**6.5 Lazy Output Flattening and Row Location**

1011 Large workbooks and selection hierarchies make fully materializing a relational view prohibitively expensive. Empirically,  
 1012 naive flattening leads to seconds or minutes of UI stalls on sheets with up to  $10^6$  rows (Excel's limit) and many columns.  
 1013 Our goal is to *render only what the user is about to see*, without precomputing the entire output.

1014

1015 *Design overview.* We model the visible table as a single *global row space* obtained by concatenating many small,  
 1016 contiguous *row blocks*. Each block is produced by streaming the hierarchy files  $\rightarrow$  tasks  $\rightarrow$  sheets  $\rightarrow$  cellTasks in  
 1017 a deterministic order. The UI asks for a particular global row index  $r$  (e.g., the first row currently in the viewport); we  
 1018 then extend the stream just far enough so that  $r$  falls inside a cached block. This *on-demand flattening* avoids touching  
 1019 unrelated parts of the hierarchy.

1020

1021 *Data structures.* We maintain two parallel arrays: (i) *blocks* contains the realized row blocks (each stores *startRow*,  
 1022 *len*, *path*, *cells*, and the active workbook/sheet), and (ii) *starts* stores the corresponding *startRow* values. By con-  
 1023 struction, *starts* is strictly increasing. A FIFO queue *Q* holds pending (*task*, *path*) frames for a breadth-first stream-  
 1024 ing traversal. Traversal indices over files/sheet-tasks/sheets maintain the current context (*activeWb*, *activeSheet*).  
 1025 Optional caps  $B_{\max}$  and  $R_{\max}$  bound memory by pruning the oldest blocks.

1026

1027 *Driver and lookup.* When the UI requests row  $r$ , *ENSUREBUILTRHROUGHRow* extends the stream until  $\text{builtRows} > r$   
 1028 or the source is exhausted (Alg. 6). We then locate the block via a binary search over *starts* (*upper bound* on  $r$  and  
 1029 step one back), yielding the block index and the local in-block offset (Alg. 6, *LOCATERow*). Both steps are  $O(k)$  work to  
 1030 extend by  $k$  newly discovered rows plus  $O(\log |starts|)$  for the lookup.

1031

1032 *Source advancement.* *FILLQUEUEIFEMPTY* (Alg. 8) advances through the outer hierarchy: it steps files (*fi*), sheet tasks  
 1033 (*sti*), then sheet pairs (*si*). For each sheet pair (*wb*, *sh*) it materializes the roots (*importExcelCellsTasks*) into *Q* and  
 1034 Manuscript submitted to ACM

1035

1036

1037

1038

1039

1040

**1041** sets the active context used to form RowBlocks. If a segment has no roots, it is skipped. When the last file is exhausted  
**1042** and  $Q$  remains empty, the function returns **false** and the stream is complete.  
**1043**

**Algorithm 8:** Traversal feeding (part C): FillQueueIfEmpty

```

1046 Function FILLQUEUEIFEMPTY:
1047   while Q =  $\emptyset$  do
1048     if curTask =  $\perp$  then
1049       if  $fi \geq |files|$  then
1050         return false
1051       curFile  $\leftarrow files[fi + 1]$ ; sti  $\leftarrow 0$ 
1052     if sti  $\geq |curFile.sheetTasks|$  then
1053       curTask  $\leftarrow \perp$ ; continue
1054     curTask  $\leftarrow curFile.sheetTasks[sti + 1]$ ; curSheets  $\leftarrow$  list( $curTask.sheets$ ); si  $\leftarrow 0$ 
1055     while si <  $|curSheets|$  and Q =  $\emptyset$  do
1056       (wb, sh)  $\leftarrow curSheets[si + 1]$ ; roots  $\leftarrow curTask.importExcelCellsTasks$ 
1057       if  $|roots| = 0$  then
1058         continue
1059       Q  $\leftarrow$  queue of  $(root, \emptyset)$  for each  $root \in roots$ 
1060       activeWb  $\leftarrow wb$ ; activeSheet  $\leftarrow sh$ 
1061     if Q  $\neq \emptyset$  then
1062       return true
1063   return true

```

*Cache pruning.* PRUNEHEADIFNEEDED (Alg. 9) trims the front of the cache to respect either (i) a block count cap  $B_{\max}$ , or (ii) a total cached row cap  $R_{\max}$ . Trimming removes the oldest blocks and their starts while preserving the invariant that `starts` remains strictly increasing and aligned with `blocks`. In practice we choose small caps that comfortably cover one or two viewport heights plus prefetch.

**Algorithm 9:** Cache pruning (part D): PruneHeadIfNeeded

```

1071
1072 Function PRUNEHEADIFNEEDED:
1073   rm  $\leftarrow$  0
1074   if  $B_{\max} \neq \perp$  and  $|blocks| > B_{\max}$  then
1075     rm  $\leftarrow |blocks| - B_{\max}$ 
1076   if  $R_{\max} \neq \perp$  then
1077     while rm  $< |blocks|$  do
1078       cached  $\leftarrow blocks[|blocks| - 1].startRow + blocks[|blocks| - 1].len - blocks[0].startRow$ 
1079       if cached  $\leq R_{\max}$  then
1080         break
1081       rm  $\leftarrow rm + 1$ 
1082   if rm  $> 0$  then
1083     drop first rm from blocks and starts
1084

```

*Invariants and correctness.* (1) **Monotone coverage:** every emitted block has  $\text{startRow} = \text{builtRows}$  at creation time, and we update  $\text{builtRows} \leftarrow \text{builtRows} + 1$ ; thus blocks are disjoint and cover  $[0, \text{builtRows})$  without gaps. (2) **Sorted index:**  $\text{starts}$  is strictly increasing; binary search always returns the last block whose  $\text{start} \leq r$ . (3) **Determinism:** the traversal order is completely determined by the order of files/sheet-tasks/sheets and by the top-down BFS over the selection tree; repeated runs produce identical global row layouts. (4) **Progress:** each child is enqueued at most once and each leaf produces at most one block; the stream terminates after a bounded number of steps.

1093 *Complexity.* Let  $N$  be the number of leaf tasks that produce non-empty `sortedSelectedCells`, and let  $M = \sum \text{len}$   
1094 be the total number of output rows. Streaming is linear in the explored work: each internal node is visited once  
1095 and each leaf contributes  $O(1)$  metadata plus  $O(\text{len})$  to copy/select references to its cells. A lookup for row  $r$  costs  
1096  $O(k + \log |\text{starts}|)$ , where  $k$  is how many *new* rows must be streamed to cover  $r$  (often  $k = 0$  for warm caches). Memory  
1097 is  $O(|\text{blocks}|)$ , bounded by  $B_{\max}$  or by  $R_{\max}$  rows of history.  
1098

1099  
1100 *UI integration.* On each frame the viewport asks for the *leading* global row (top-left visible), calls `LOCATEROW` to  
1101 obtain the block and local offset, and renders from there. We prefetch just beyond the viewport by requesting the row  
1102 at  $y_0 + H_{\text{vp}} + \Delta$ , which amortizes the streaming cost without over-allocating memory. When the user scrolls back,  
1103 previously cached blocks are reused; otherwise the binary search still runs in logarithmic time.  
1104

1105  
1106 *Failure modes.* Segments with empty selections yield no blocks but are skipped efficiently. If the hierarchy ends  
1107 before covering the requested row, the driver returns  $\perp$ ; the UI interprets this as “no more data.” All pruning policies  
1108 preserve correctness: they only remove *past* blocks and never create gaps inside the realized suffix.  
1109

1110 By applying this method, we render only the cells necessary for the current view, thereby optimizing performance  
1111 and ensuring smooth user interactions even with large and complex worksheets.  
1112

## 1113 7 Evaluation

1114 The Spreadsheet Data Extractor (SDE) builds on the converter by Aue et al. [4], whose extraction effectiveness was  
1115 evaluated on over 500 Excel files (331 files; 3,093 worksheets; mean 15 min per file, 95 s per worksheet). Our contribution  
1116 focuses on *user experience* and *latency*: we render worksheets as they appear in Excel, reduce context switching by  
1117 integrating selection hierarchy, worksheet view, and output preview, and engineer incremental loading, byte-level  
1118 parsing and plus viewport-bounded rendering.  
1119

### 1120 7.1 Acceleration When Opening Files

1121 We quantify opening latency in two complementary scenarios: (i) a *user-centred* case that measures time-to-first-visual  
1122 when opening a *selected worksheet* from a large, multi-worksheet workbook; and (ii) a *workload-equivalent* case that  
1123 uses a single worksheet with 1,048,548 rows to align the amount of work across programmes (first rows vs. last row).  
1124 Throughout, we report medians over repeated runs and show distributions as box plots on a  $\log_{10}$  time axis.  
1125

1126 *Setup.* We evaluate three programmes: the *SDE*, Microsoft Excel (automated via PowerShell/COM), and a Dart *excel*  
1127 package. Each condition was repeated ten times *unless noted otherwise*.  
1128

1129 *User-centred latency: opening a selected worksheet.* Opening a selected worksheet from a large real-world work-  
1130 book [19], SDE initialises only the requested sheet and achieves a median of **0.657 s**, compared to **45.843 s** for Excel—a  
1131 **69.8×** speedup (Fig. 11a). The Dart *excel* package completed only the first run at 343.568 s; runs 2–10 terminated with  
1132 out-of-memory on our test machine ( $n=1$ ). Based on that single run, SDE is **522.9×** faster in this scenario.  
1133

1134 *Controlling for workload comparability.* The multi-worksheet experiment reflects an important user scenario (time-to-  
1135 first-visual for a selected sheet), but it is not a like-for-like comparison: SDE initialises only the requested worksheet,  
1136 whereas the baselines initialise the entire workbook. To control for this confound and establish workload equivalence,  
1137 we construct a *single-worksheet* benchmark from the example in Section 3 (Design Philosophy) by pruning the workbook  
1138 to one sheet and duplicating the table vertically until no additional table fits, yielding 1,048,548 rows of real data. The  
1139 Manuscript submitted to ACM  
1140  
1141  
1142  
1143  
1144

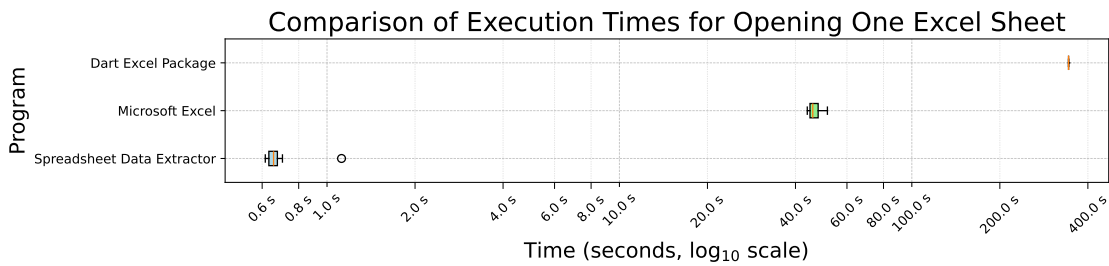
1145 resulting file is  $\sim 35$  MB on disk (XLSX ZIP container) and  $\sim 282$  MB uncompressed. We then report two cases—*first*  
 1146 *rows* (time-to-first-visual) and *last row* (forces a full parse)—to align SDE’s measured cost with eager parsers. Under  
 1147 these identical I/O and parsing conditions, SDE achieves **1.229 s** vs. **52.756 s** for Excel on first rows (**42.9 $\times$** ), and **5.515 s**  
 1148 vs. **52.228 s** on the last row (**9.47 $\times$** ).  
 1149

1150     *Results (overview).* Initialising only the selected sheet yields much lower time-to-first-visual (Fig. 11a); under identical  
 1151 workload SDE remains  $\sim 10\times$  faster even when a full parse is enforced (Fig. 11b).  
 1152

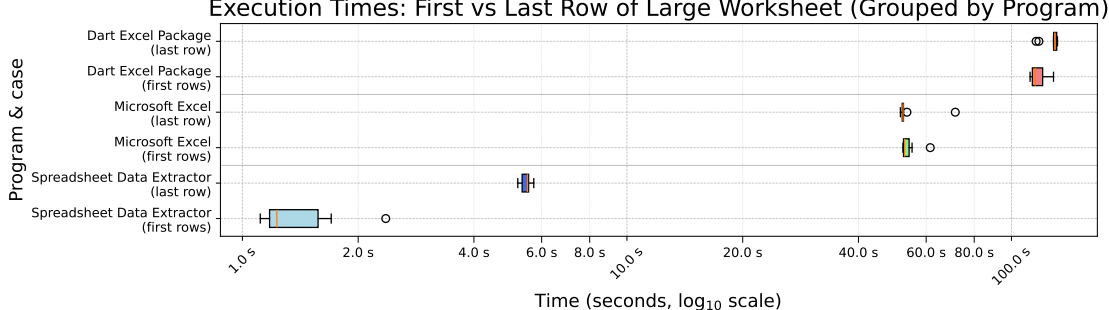
## 1153 7.2 Interactive scalability

1154 While the underlying extraction model remained effective, the previous prototype did not stay interactive on very large  
 1155 sheets. Empirically, on workbooks with hundreds of thousands of rows—and in particular near Excel’s  $10^6$ -row limit—  
 1156 two failure modes dominated:  
 1157

- 1158 (1) **Eager materialisation in views.** When the selection view or the output view attempted to realise large regions  
     eagerly, per-frame times rose above 1 s, making panning and selection unusable.
- 1159 (2) **Large selection hierarchies.** With many nested selections, highlight updates and duplicate/move previews  
     performed work proportional to the total number of selected cells, causing multi-second pauses per interaction  
     and making operations on large datasets impractical.



(a) Large multi-worksheet workbook: opening one selected sheet (user-centred latency).



(b) Single-worksheet benchmark (1,048,548 rows): first vs. last row per programme.

1193 Fig. 11: Time-to-first-visual vs. full-parse costs across tools. (a) shows the practical benefit of initialising only the selected  
 1194 sheet in a multi-worksheet file; (b) isolates algorithmic differences under identical workload. Both plots aggregate 10  
 1195 runs on a logarithmic time axis.  
 1196



Fig. 12: SDE performance profiling during scrolling. Timeline shows per-frame rendering costs (blue); average 18ms/frame and peak 54ms/frame.

These observations motivated the engineering in 6.2 Parsing Worksheet XML with Byte-Level Pattern Matching: (i) byte-level, on-demand parsing of worksheet XML; (ii) viewport-bounded rendering that lays out only  $[r_l : r_u] \times [c_l : c_u]$  (Algorithm Two-Dimensional Grid Viewport Rendering); (iii) AABB-based filtering of selection sources with cache invalidation (6.4 AABB-Indexed Selection Lookup); and (iv) on-demand flattening of the output table (6.5 Lazy Output Flattening and Row Location). Together these changes bound per-interaction work to the visible area rather than the sheet size.

On a sheet with  $10^6$  rows and a selection covering all cells, the UI remained smooth during scrolling, sustaining  $\approx 2$  ms per frame (Fig. 12), which corresponds to  $\approx 500$  FPS. When dragging the scrollbar—filling the entire viewport at once with new content—frame times rose to about 60-80 ms ( $\approx 12\text{-}17$  FPS), which remained acceptable for rapid navigation at that scale.

*Benchmarking environment.* All tests were conducted on a machine with an AMD Ryzen 5 PRO 7535U with Radeon Graphics (6-core CPU at 2.9 GHz), 31.3 GB RAM, and a hard disk drive (HDD), running Microsoft Windows 11 Enterprise (build 26100, 64-bit). The version of Microsoft Excel used was version 16.0.

## 8 Artifact Availability

All code, benchmark scripts, Excel automation, input workbooks, and chart generators are available in an anonymized repository during review: <https://anonymous.4open.science/r/spreadsheet-data-extractor-paper-3CF0/>. The package includes a step-by-step README and VS Code launch configurations to reproduce all timings and figures.

## 9 Conclusion

In this paper, we introduced the Spreadsheet Data Extractor [2], an enhanced tool that builds upon the foundational work of Aue et al. [4]. By addressing key limitations of the existing solution, we implemented significant performance optimizations and usability enhancements. Specifically, SDE employs incremental loading of worksheets and optimizes rendering by processing only the visible cells, resulting in performance improvements that enable the tool to open large Excel files.

We also integrated the selection hierarchy, worksheet view, and output preview into a unified interface, streamlining the data extraction process. By adopting a user-centric approach that gives users full control over data selection and metadata hierarchy definition without requiring programming knowledge, we provide a robust and accessible solution for data extraction. Our tool offers user-friendly features such as the ability to duplicate hierarchies of columns and tables and to move them over similar structures for reuse, reducing the need for repetitive configurations.

By combining the strengths of the original approach with our enhancements in user interface and performance optimizations, our tool significantly improves the efficiency and reliability of data extraction from diverse and complex spreadsheet formats.

## 1249 References

- 1250 [1] Rui Abreu, Jácrome Cunha, Joao Paulo Fernandes, Pedro Martins, Alexandre Perez, and Joao Saraiva. 2014. Faultysheet detective: When smells meet  
1251 fault localization. In *2014 IEEE International Conference on Software Maintenance and Evolution*. IEEE, 625–628.
- 1252 [2] Anonymous. [n. d.]. Spreadsheet Data Extractor (SDE). [https://anonymous.4open.science/r/spreadsheet\\_data\\_extractor-13BD/README.md](https://anonymous.4open.science/r/spreadsheet_data_extractor-13BD/README.md).  
1253 Accessed: 2024-12-08.
- 1254 [3] Anonymous. 2025. Spreadsheet Data Extractor (SDE): Artifact and Reproduction Package. <https://anonymous.4open.science/r/spreadsheet-data-extractor-paper-3CF0/>. Anonymized repository for review; a citable DOI will be added upon acceptance.
- 1255 [4] Alexander Aue, Andrea Ackermann, and Norbert Röder. 2024. Converting data organised for visual perception into machine-readable formats. In *44.  
1256 GIL-Jahrestagung, Biodiversität fördern durch digitale Landwirtschaft*. Gesellschaft für Informatik eV, 179–184.
- 1257 [5] Daniel W Barowy, Sumit Gulwani, Ted Hart, and Benjamin Zorn. 2015. FlashRelate: extracting relational data from semi-structured spreadsheets  
1258 using examples. *ACM SIGPLAN Notices* 50, 6 (2015), 218–228.
- 1259 [6] D.J. Berndt, J.W. Fisher, A.R. Hevner, and J. Studnicki. 2001. Healthcare data warehousing and quality assurance. *Computer* 34, 12 (2001), 56–65.  
1260 doi:10.1109/2.970578
- 1261 [7] Zhe Chen, Michael Cafarella, Jun Chen, Daniel Prevo, and Junfeng Zhuang. 2013. Senbazuru: A prototype spreadsheet database management  
1262 system. *Proceedings of the VLDB Endowment* 6, 12, 1202–1205.
- 1263 [8] Jácrome Cunha, Joao Paulo Fernandes, Pedro Martins, Jorge Mendes, and Joao Saraiva. 2012. Smellsheet detective: A tool for detecting bad smells in  
1264 spreadsheets. In *2012 IEEE Symposium on Visual Languages and Human-Centric Computing (VL/HCC)*. IEEE, 243–244.
- 1265 [9] Kaval Desai. 2024. Excel Dart Package. <https://pub.dev/packages/excel>. Accessed: 2024-12-03.
- 1266 [10] Haoyu Dong, Shijie Liu, Shi Han, Zhouyu Fu, and Dongmei Zhang. 2019. Tablesense: Spreadsheet table detection with convolutional neural  
1267 networks. In *Proceedings of the AAAI conference on artificial intelligence*, Vol. 33, 69–76.
- 1268 [11] Angus Dunn. 2010. Spreadsheets-the Good, the Bad and the Downright Ugly. *arXiv preprint arXiv:1009.5705* (2010).
- 1269 [12] Julian Eberius, Christopher Werner, Maik Thiele, Katrin Braunschweig, Lars Dannecker, and Wolfgang Lehner. 2013. DeExcelerator: a framework for  
1270 extracting relational data from partially structured documents. In *Proceedings of the 22nd ACM international conference on Information & Knowledge  
Management*, 2477–2480.
- 1271 [13] Elvis Koci, Dana Kuban, Nico Luettig, Dominik Olwig, Maik Thiele, Julius Gonsior, Wolfgang Lehner, and Oscar Romero. 2019. Xlindy: Interactive  
1272 recognition and information extraction in spreadsheets. In *Proceedings of the ACM Symposium on Document Engineering 2019*. 1–4.
- 1273 [14] Kate Lovett. 2023. two\_dimensional\_scrollables package - Commit 4c16f3e. <https://github.com/flutter/packages/commit/4c16f3ef4033aa0aebe8a1e46ef7b9fef9a1c1f> Accessed: 2023-08-17.
- 1274 [15] Kelly Mack, John Lee, Kevin Chang, Karrie Karahalios, and Aditya Parameswaran. 2018. Characterizing scalability issues in spreadsheet software  
1275 using online forums. In *Extended Abstracts of the 2018 CHI Conference on Human Factors in Computing Systems*. 1–9.
- 1276 [16] Sajjadur Rahman, Mangesh Bendre, Yuyang Liu, Shichu Zhu, Zhaoyuan Su, Karrie Karahalios, and Aditya G Parameswaran. 2021. NOAH: interactive  
1277 spreadsheet exploration with dynamic hierarchical overviews. *Proceedings of the VLDB Endowment* 14, 6 (2021), 970–983.
- 1278 [17] Gursharan Singh, Leah Findlater, Kentaro Toyama, Scott Helmer, Rikin Gandhi, and Ravin Balakrishnan. 2009. Numeric paper forms for NGOs. In  
1279 *2009 International Conference on Information and Communication Technologies and Development (ICTD)*. IEEE, 406–416.
- 1280 [18] Statistisches Bundesamt (Destatis). 2024. *Statistischer Bericht - Pflegekräftevorausberechnung - 2024 bis 2070*. Technical Report. Statistisches  
1281 Bundesamt, Wiesbaden, Germany. <https://www.destatis.de/DE/Themen/Gesellschaft-Umwelt/Bevoelkerung/Bevoelkerungsvorausberechnung/Publikationen/Downloads-Vorausberechnung/statistischer-bericht-pflegekraeftevorausberechnung-2070-5124210249005.html> Statistical Report -  
1282 Projection of Nursing Staff - 2024 to 2070.
- 1283 [19] Statistisches Bundesamt (Destatis). 2024. Statistischer Bericht: Rechnungsergebnis der Kernhaushalte der Gemeinden. <https://www.destatis.de/DE/Themen/Staat/Oeffentliche-Finanzen/Ausgaben-Einnahmen/Publikationen/Downloads-Ausgaben-und-Einnahmen/statistischer-bericht-rechnungsergebnis-kernhaushalt-gemeinden-2140331217005.html> Accessed: 2024-11-29.
- 1284 [20] Alaaeddin Swidan, Felienné Hermans, and Ruben Koesoemowidjojo. 2016. Improving the performance of a large scale spreadsheet: a case study. In  
1285 *2016 IEEE 23rd International Conference on Software Analysis, Evolution, and Reengineering (SANER)*, Vol. 1. IEEE, 673–677.
- 1286 [21] Dixin Tang, Fanchao Chen, Christopher De Leon, Tana Wattanawaroon, Jeaseok Yun, Srinivasan Seshadri, and Aditya G Parameswaran. 2023.  
Efficient and Compact Spreadsheet Formula Graphs. In *2023 IEEE 39th International Conference on Data Engineering (ICDE)*. IEEE, 2634–2646.
- 1287 [22] Hannah West and Gina Green. 2008. Because excel will mind me! the state of constituent data management in small nonprofit organizations. In  
1288 *Proceedings of the Fourteenth Americas Conference on Information Systems*. Association for Information Systems, AIS Electronic Library (AISeL).  
1289 <https://aisel.aisnet.org/amcis2008/336>